Original Research Article

In Situ Mapping of the Glucose Metabolism Heterogeneity in Atherosclerosis: Correlation With 2-Deoxyglucose Uptake

Molecular Imaging
Volume 23: 1–10

DOI: 10.1177/15353508241280573
journals.sagepub.com/home/mix
Sage

Joseph Haddad, MD[1,*], Selim Demirdelen, MD[1,*], Clayton E. Barnes, BS[1], Steven A. Leers, MD[2] and Sina Tavakoli, MD, PhD[1,3,4]

Abstract

Objective: 2-Deoxy-2-[^{18}F]fluoro-D-glucose ([^{18}F]FDG) is widely used for noninvasive imaging of atherosclerosis. However, knowledge about metabolic processes underlying [^{18}F]FDG uptake is mostly derived from *in vitro* cell culture studies, which cannot recapitulate the complexities of the plaque microenvironment. Here, we sought to address this gap by *in situ* mapping of the activity of selected major dehydrogenases involved in glucose metabolism in atherosclerotic plaques.

Methods: *In situ* activity of lactate dehydrogenase (LDH), glucose-6-phosphate dehydrogenase (G6PD), succinate dehydrogenase (SDH), and isocitrate dehydrogenase (IDH) was assessed in plaques from murine aortic root and brachiocephalic arteries and human carotid arteries. High-resolution 2-deoxy-D-[1,2-^{3}H]glucose ([^{3}H]2-deoxyglucose) autoradiography of murine brachiocephalic plaques was performed.

Results: LDH activity was heterogeneous throughout the plaques with the highest activity in medial smooth muscle cells (SMCs). G6PD activity was mostly confined to the medial layer and to a lesser extent to SMCs along the fibrous cap. SDH and IDH activities were minimal in plaques. Plaque regions with increased [^{3}H]2-deoxyglucose uptake were associated with a modestly higher LDH, but not G6PD, activity.

Conclusions: Our study reveals a novel aspect of the metabolic heterogeneity of the atherosclerotic plaques, enhancing our understanding of the complex immunometabolic biology that underlies [^{18}F]FDG uptake in atherosclerosis.

Keywords

atherosclerosis, metabolism, [^{18}F]FDG, macrophage, vascular smooth muscle cell

Received May 28, 2024; Revised July 10, 2024; Accepted for publication July 19, 2024

Introduction

Metabolic imaging of atherosclerosis by positron emission tomography (PET) has been extensively investigated, aiming to enhance plaque characterization and predict the risk of vulnerability beyond what can be achieved by conventional imaging methods which primarily focus on detecting the severity of luminal stenosis.[1] In addition to supporting the bioenergetics and biomass demands, metabolism regulates diverse functions of cells residing within the atherosclerotic plaques, such as the leukocytes' response to inflammatory stimuli.[1,2] However, the metabolic states of the cells involved in atherogenesis have been mostly explored using *in vitro*

[1]Departments of Radiology, Division of Cardiothoracic Imaging, University of Pittsburgh, Pittsburgh, PA, USA
[2]Departments of Surgery, Division of Vascular Surgery, University of Pittsburgh, Pittsburgh, PA, USA
[3]Departments of Medicine, Division of Cardiology, University of Pittsburgh, Pittsburgh, PA, USA
[4]Heart, Lung, Blood, and Vascular Medicine Institute, UPMC Department of Medicine, Pittsburgh, PA, USA

[*]These authors contributed equally to this manuscript.

Corresponding Author:
Sina Tavakoli, Department of Radiology, University of Pittsburgh Medical Center (UPMC), Eye and Ear Institute, 203 Lothrop Street, Suite 700, Pittsburgh, PA 15213, USA.
Email: sit23@pitt.edu

culture conditions, which cannot recapitulate the complexities of the plaque microenvironment.[1,2] While 2-deoxy-2-[^{18}F]fluoro-D-glucose ([^{18}F]FDG) PET allows for *in vivo* detection of metabolism, its low spatial resolution precludes accurate mapping of the heterogeneities across different plaque components.[1] Moreover, the biological correlates of [^{18}F]FDG uptake in atherosclerosis have remained incompletely understood.[1] For example, while enhanced glycolytic activity of proinflammatory macrophages has been considered as the primary driver of [^{18}F]FDG uptake in atherosclerotic plaques,[1] recent studies have suggested that other cell types, particularly smooth muscle cells (SMC),[3,4] or other activation states of macrophages[5,6] may significantly contribute to [^{18}F]FDG uptake. Additionally, the association between [^{18}F]FDG uptake and intracellular utilization of glucose through different metabolic pathways has not been studied within the plaque microenvironment.

Most of the literature on the contribution of different cell types to [^{18}F]FDG uptake in atherosclerosis is based on *in vitro* metabolic studies of SMCs and macrophages cultured in the presence of various chemokines, growth factors, or environmental stimuli (eg, hypoxia, oxidized low-density lipoproteins, and lipopolysaccharide).[1,5–10] However, these conditions do not accurately replicate the complex microenvironment of the vessel wall.[1] While alternative approaches such as transcriptomics, proteomics, and metabolomics analysis of tissue lysates have been utilized, these methods do not assess the heterogeneity of the cellular metabolism within tissues.[11] Additionally, the regulation of metabolic enzyme activity is markedly influenced by posttranscriptional and posttranslational mechanisms, which cannot be adequately assessed by transcriptional and proteomics approaches.[12] To address the knowledge gaps in metabolic assessment of cells within the native microenvironment of plaques, we employed *in situ* enzyme histochemistry technique to provide a high-resolution map of the activity of selected key dehydrogenases involved in glucose metabolism in murine and human atherosclerotic plaques. By applying the metabolic substrates of specific enzymes of interest along with a chromogenic substrate, this technique allows for visualization and quantitative assessment of the enzymatic activities of different cell types within their native tissue microenvironment.[12] This technique has been previously used to reveal the metabolic heterogeneity of neoplastic tissues,[11,12] but to our knowledge the current study represents its first report in atherosclerosis. Our results demonstrated a significant heterogeneity in the activity of the selected dehydrogenases in three major glucose utilization pathways, including: (1) lactate dehydrogenase (LDH, a critical enzyme for the continuation of glycolytic activity through regeneration of nicotinamide adenine dinucleotide [NAD^+][13]); (2) glucose-6-phosphate dehydrogenase (G6PD, a rate-limiting enzyme in pentose phosphate pathway [PPP][14]); and (3) succinate dehydrogenase (SDH) and isocitrate dehydrogenase (IDH) (critical enzymes in tricarboxylic acid (TCA) cycle). We also examined the relationship between LDH and G6PD activities with the uptake of 2-deoxy-D-[1,2-^{3}H]glucose ([^{3}H]2-deoxyglucose), as a surrogate for [^{18}F]FDG, in murine brachiocephalic artery plaques.

Methods

Mouse Model of Atherosclerosis

Apolipoprotein E knockout ($apoE^{-/-}$) mice (N = 9, 3 males and 6 females) on C57BL/6J background (Jackson Laboratories) were fed by an atherogenic western diet (21% anhydrous fat, TD88137, Envigo). Mice were euthanized at ~3 months (early plaques) or ~7 months (advanced plaques) after western diet feeding. Aortic roots and brachiocephalic arteries were excised for histological and autoradiographic experiments. Experiments were conducted in accordance with a protocol approved by the University of Pittsburgh Institutional Animal Care and Use Committee.

Immunofluorescent Staining of Murine Atherosclerotic Plaques

Unfixed 10-μm thick plaque cryosections were stained for CD68 and α-smooth muscle actin (α-SMA), as surrogates for monocytes/macrophages and SMC, respectively, using commercially available antibodies (Supplemental Table 1). Tissues were temporarily mounted using ProLong™ Gold Antifade containing 4′,6-diamidino-2-phenylindole (DAPI, Invitrogen). Fluorescent images were acquired using an Axiovert 200 inverted microscope (Zeiss) equipped with a digital camera, controlled by ZEN software (Zeiss).

In Situ Enzyme Histochemistry

After the acquisition of immunofluorescent images, coverslips were removed by submerging the slides in PBS for subsequent mapping of the activity of 4 selected enzymes catalyzing key steps in glucose metabolism, ie, LDH, G6PD, SDH, and IDH, according to previously described methods[11,12] with minor modifications. Tissues were incubated with enzyme-specific buffers (Supplemental Table 2) at 37 °C to allow for *in situ* formation and precipitation of blue-colored formazan at sites of the enzymatic activity.[11,12] After washing, tissues were dehydrated and cleared in xylene and permanently mounted using (VectaMount mounting medium, Vector labs). Brightfield images were acquired using an Axiovert 200 microscope.

Quantification Technique

For quantification of enzymatic activity in different cell types, the corresponding immunostaining (fluorescent) and enzyme histochemistry (brightfield) images were overlaid and image layers were converted into a grayscale format. Two mask layers were manually drawn to define the total vessel wall and the medial layer (Supplemental Figure 1).

A grid was then applied to the overlaid fluorescent and brightfield images to record the intensity of CD68, α-SMA, and the enzyme activity in each 13×13 μm square of the grid (Azure software). These multiparametric data were then imported to FlowJo software to analyze enzymatic activities in CD68-positive and α-SMA-positive regions of the medial and intimal layers of the vessel wall. Enzymatic activities were reported after correcting for background (ie, signal from negative control slides incubated with the buffers lacking the metabolic substrates) and normalization to standard curves (prepared by adding known amounts of enzymes to assay buffers) to account for batch-to-batch variations in enzyme assay buffers. Quantifications of enzymatic activities were performed on 2-3 tissue sections per mouse as technical replicates, and the average values were used as biological replicates.

Immunohistochemistry and Enzyme Histochemistry of Human Carotid Endarterectomy Specimens

Anonymized atherosclerotic plaques were collected from 3 patients who underwent standard-of-care carotid endarterectomy under a "No Human Subject involvement" classification by the University of Pittsburgh Institutional Review Board. Considering the No Human Subject designation, informed consent was not required for this study. Immunohistochemical staining was performed by incubation of 10-μm thick cryosections with anti-CD68 or anti-α-SMA antibodies followed by horseradish peroxidase-conjugated secondary antibodies (Supplemental Table 1) for chromogenic detection (to avoid the high autofluorescence of human plaques). Tissues adjacent to CD68 and α-SMA stained slides were used for *in situ* enzyme histochemistry, as described above.

High-Resolution [^{3}H]2-Deoxyglucose Autoradiography of Murine Atherosclerotic Plaques

Excised brachiocephalic arteries were incubated in a glucose-free uptake buffer (NaCl: 140 mM, KCl: 5.4 mM, $CaCl_2$: 1.8 mM, $MgSO_4$: 0.8 mM, HEPES: 25 mM),[8] supplemented by 40 μCi/mL (1.48 MBq/mL) of [^{3}H]2-deoxyglucose (American Radiolabeled Chemicals Inc., ART-0103A) at 37 °C for 2 h. Subsequently, arteries were washed with a cold buffer and embedded in optimal cutting temperature (OCT) compound and cryo-sectioned (Leica CM1860) at 10-μm thickness. Tissues were exposed to tritium-sensitive BAS storage phosphor screens (BAS-IP TR 2025e, GE Healthcare) for 3-4 weeks at −20 °C. Phosphor screens were scanned by a Sapphire Biomolecular Imager (Azure Biosystems) at 20-μm resolution. Tissues were then used for immunostaining and enzyme histochemistry, as described above. The average intensity of enzyme activities was calculated in different quartiles of [^{3}H]2-deoxyglucose uptake. Representative autoradiography images are shown after adjustment by the Fire Look-Up Table and smoothing algorithm (Image J).

Statistical Analysis

Statistical analysis was performed using GraphPad Prism software (version 8). Data are presented as mean ± SEM. Mean values between experimental groups were compared using a one-way analysis of variance (ANOVA) followed by Fisher's Exact *post hoc* test. $P < .05$ was considered statistically significant.

Results

Metabolic Heterogeneity of Murine Atherosclerotic Plaques

The visual assessment of the murine aortic roots demonstrated heterogenous levels of LDH activity within the intimal and medial layers (Figure 1A). On the other hand, G6PD activity was mostly confined to the media and to a lesser extent along the fibrous caps of plaques (Figure 1B). Notably, the activity of the two TCA cycle dehydrogenases, ie, SDH (Figure 1C) and IDH (Supplemental Figure 2), were minimal within the intimal and medial layers as opposed to the intense activity of the adjacent myocardium.

Quantification of LDH Activity in Murine Aortic Root Plaques

We next compared the LDH activity in macrophages and SMCs, as two highly abundant cell types with key functions in atherogenesis. The LDH was selected as a surrogate to assess the glycolytic flux within the vessel wall, considering its critical role in sustaining the glycolysis through the reoxidation of NADH to NAD^+ during the conversion of pyruvate to lactate.[15,16] To this end, we performed sequential immunofluorescent staining for CD68 and α-SMA followed by *in situ* enzyme histochemistry of the same tissue sections to allow for their co-registration (Figure 2A). Quantitative analysis demonstrated that LDH activity was ~50% higher in medial α-SMA$^+$ regions compared to intimal α-SMA$^+$ and CD68$^+$ regions (Figure 2B-E) in both early and advanced plaques (~3 *vs.* 7 months of western diet). Moreover, LDH activity of all 3 populations was significantly lower in advanced compared to early plaques.

Quantification of G6PD Activity in Murine Aortic Root Plaques

Consistent with the visual assessment (Figure 3A), G6PD activity was markedly higher in the medial α-SMA$^+$ regions compared to the intimal α-SMA$^+$ (~6-fold) and CD68$^+$ (~7-fold) regions (Figure 3B-E) both in early and advanced plaques. Most intimal α-SMA$^+$ cells demonstrated no or negligible

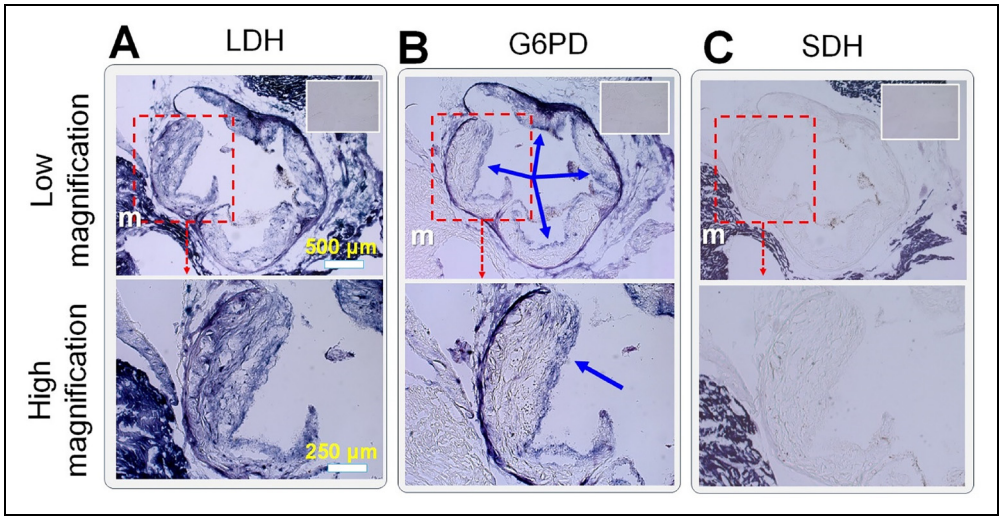

Figure 1. *In situ* metabolic mapping of atherosclerotic plaques. Representative low-magnification (top) and high-magnification (bottom) *in situ* enzyme histochemistry images from aortic root plaques of apoE$^{-/-}$ mice ~7 months after western diet feeding. **(A)** A heterogeneously high LDH activity is present within the media and intima. **(B)** G6PD activity is mostly confined to the media and to a lesser extent along the fibrous cap (blue arrows). G6PD activity is substantially lower in the myocardium (white "m") compared to the vessel wall. **(C)** SDH activity is minimal in both intima and media in contrast to intense activity of the myocardium. Insets represent negative controls performed in the presence of chromogenic substrate and other reaction constituents except for the relevant metabolic substrates (ie, lactate, glucose-6-phosphate, and succinate).

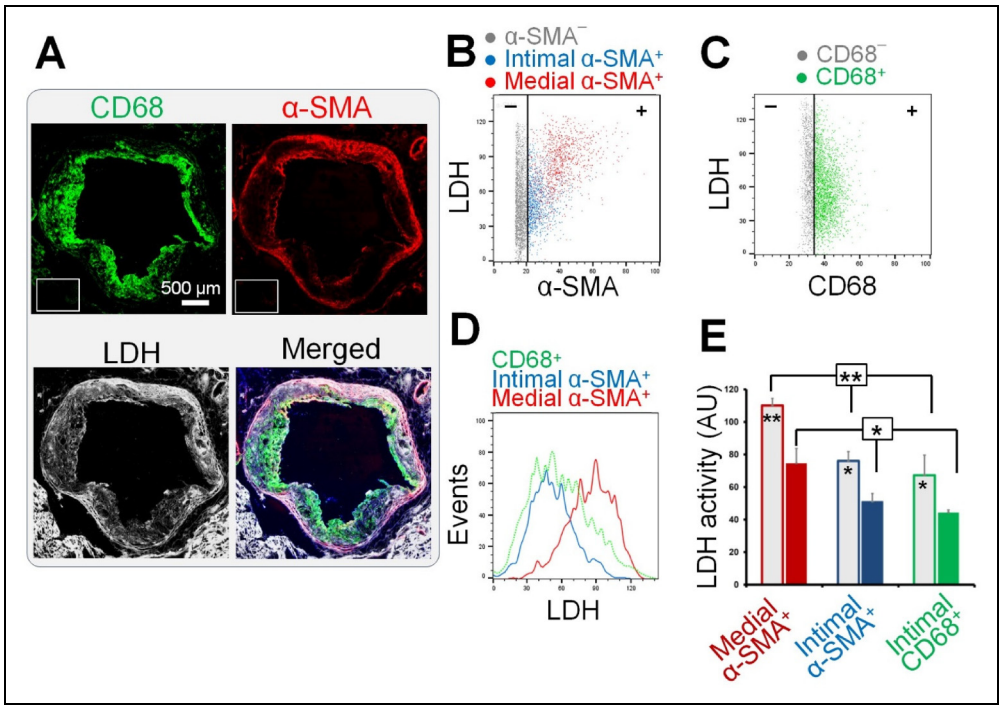

Figure 2. Quantification of LDH activity of plaque macrophages and smooth muscle cells. **(A)** Representative CD68 and α-SMA immunostaining and coregistered LDH *in situ* histochemistry images. Quantification of background-corrected LDH activity versus the intensity of CD68 **(B)** and α-SMA **(C)** expression in 13 × 13 µm grid boxes. **(D)** Representative histograms and **(E)** the average ± SEM bar charts of LDH activity in CD68 versus intimal and medial α-SMA positive regions. Empty and filled bars in panel E represent early (~3 months) and advanced (~7 months) plaques. There is an overall ~50% higher LDH activity within medial α-SMA$^+$ regions compared to intimal α-SMA$^+$ and CD68$^+$ regions, though significant heterogeneity and overlaps exist in LDH activity among these regions both in the intima and media. Additionally, early plaques had a higher LDH activity in CD68$^+$ and α-SMA$^+$ (both intimal and medial) regions compared to the advanced plaques. $N = 8$-9 plaques from 3 mice at ~3 months and 3 mice at ~7 months after western diet. *: $P < .05$, **: $P < .01$ by one-way analysis of variance (ANOVA) followed by Fisher's LSD *post hoc* test. Asterisks within the bars denote P values from a comparison of enzymatic activity of each cell type between 3 and 7 months. P values from the comparison between different components are shown above the graphs.

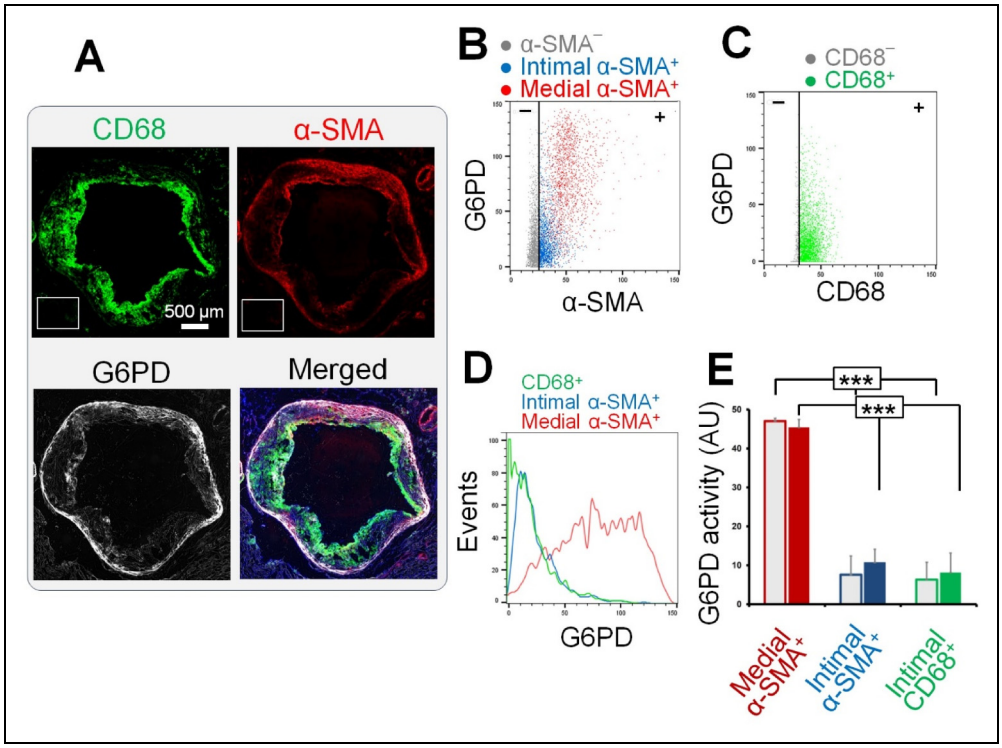

Figure 3. Quantification of G6PD activity of plaque macrophages and smooth muscle cells. **(A)** Representative CD68 and α-SMA immunostaining and coregistered G6PD *in situ* histochemistry images. Quantification of background-corrected G6PD activity versus the intensity of α-SMA **(B)** and CD68 **(C)** expression. In contrast to the LDH activity, G6PD activity was mostly confined to medial α-SMA$^+$ regions with substantially less overlap between the activity of media and intima except for modest G6PD activities along the fibrous cap as demonstrated by the representative histograms **(D)** and the bar chart **(E)**. G6PD activity of α-SMA$^+$ and CD68$^+$ cells was comparable between the early and advanced plaques. Empty and filled bars in panel E represent early (~3 months) and advanced (~7 months) plaques. *N* = 8-9 plaques from 3 mice at ~3 months and 3 mice at ~7 months after western diet. ***: $P < .001$ by one-way analysis of variance (ANOVA) followed by Fisher's LSD *post hoc* test.

G6PD activity except for small populations of α-SMA$^+$ intimal cells with moderate G6PD activity along the fibrous cap. Unlike LDH, there was no difference in the G6PD activity of α-SMA$^+$ and CD68$^+$ cells between the early and advanced plaques.

Metabolic Heterogeneity of Human Carotid Plaques

To address the translational relevance of the observed metabolic heterogeneity of murine atherosclerosis plaques, we qualitatively assessed the *in situ* activity of the LDH and G6PD in human carotid endarterectomy specimens. Consistent with our findings in murine aortic root plaques, a heterogeneous LDH activity was present within both intima and media (Figure 4A), whereas the G6PD activity was primarily localized to α-SMA$^+$ cells within the media and to a lesser extent along the fibrous caps (Figure 4B).

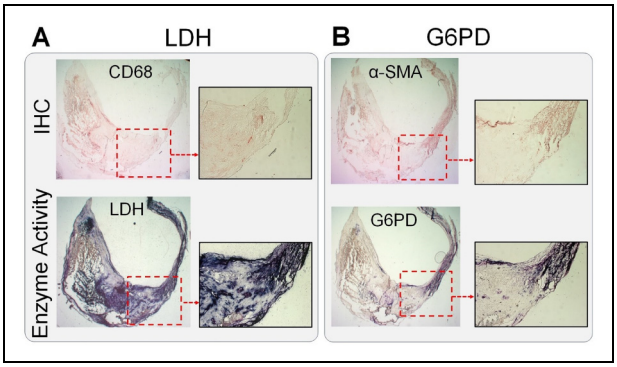

Figure 4. *In situ* metabolic mapping of atherosclerotic plaques. Consistent with the observed patterns in murine atherosclerotic plaques, human carotid endarterectomy specimens demonstrated a high, but markedly heterogeneous, level of LDH activity **(A)** within both media and intima, as opposed to G6PD activity **(B)** which was mostly restricted to the media and fibrous cap ($N = 3$).

Spatial Correlation of LDH and G6PD Activity with [^{3}H]2-Deoxyglucose Uptake

We next determined if [^{3}H]2-deoxyglucose autoradiography, as a high-resolution surrogate for [^{18}F]FDG PET, distinguishes plaque regions with different levels of LDH and G6PD activity. To avoid scattered radiation from myocardium which interferes with an accurate quantification of

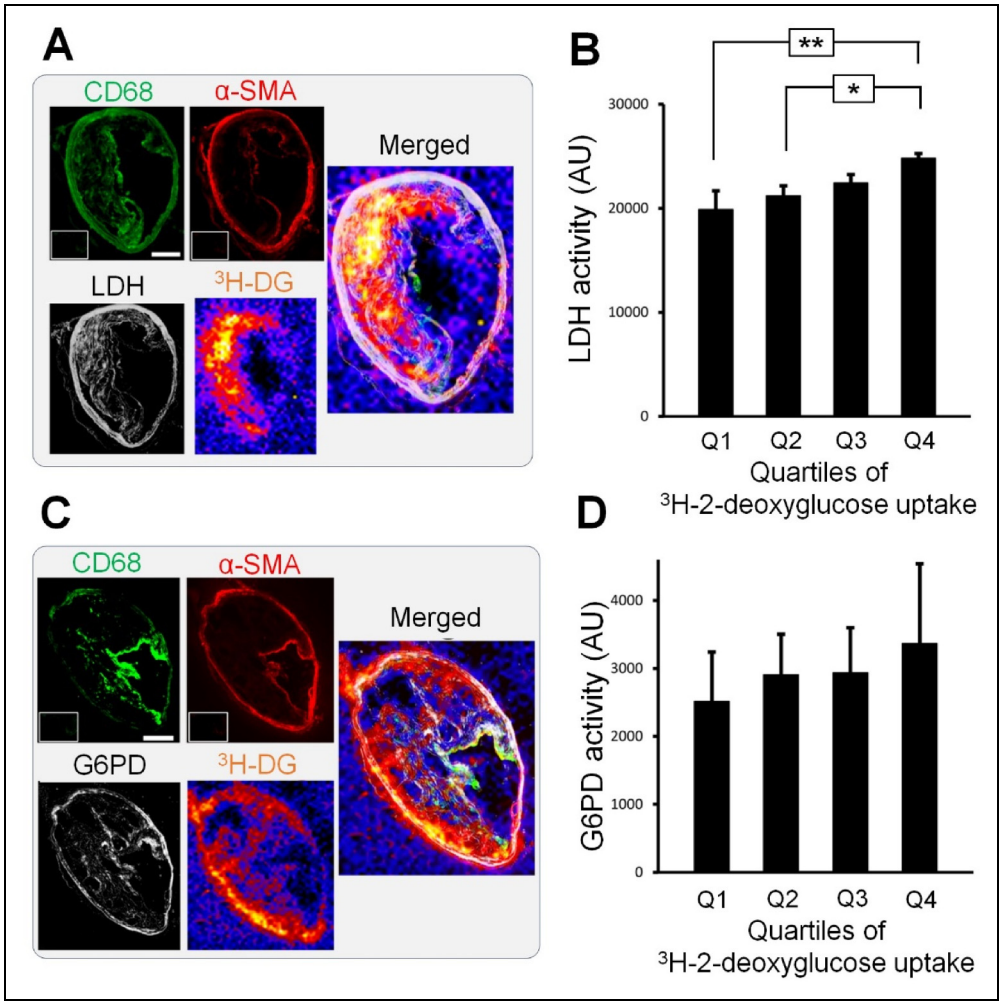

Figure 5. Combined high-resolution [^{3}H]2-deoxyglucose autoradiography and enzyme histochemistry of murine brachiocephalic plaques. Combined immunostaining, enzyme histochemistry, and high-resolution autoradiography (Fire Look-Up Table and smoothing algorithm, Image J) of advanced murine brachiocephalic artery plaques was performed to determine if glucose uptake correlates with LDH **(A-B)** and G6PD **(C-D)** activities of plaques. Representative imaging (A and C) and quantification of superimposed images using overlaid grids (B and D) demonstrate a progressive, but modest, increase in LDH activity in regions with higher [^{3}H]2-deoxyglucose uptake (B) ($N = 18$ plaques from 3 mice). However, G6PD activity was not statistically different across different quartiles of [^{3}H]2-deoxyglucose uptake (D) ($N = 14$ plaques from 3 mice). Q1 to Q4: lowest to highest quartiles of [^{3}H]2-deoxyglucose uptake.

glucose uptake in the aortic root, we used brachiocephalic plaques from apoE$^{-/-}$ mice after 7 months of western diet feeding. A modest incremental increase in LDH activity was present across regions of plaques with increased [^{3}H] 2-deoxyglucose uptake which reached ~25% higher activity in the highest quartile compared to the lowest quartile (Figure 5A-B). However, G6PD activity was comparable across different quartiles of [^{3}H]2-deoxyglucose uptake (Figure 5C-D).

Discussion

This study uncovered distinct patterns of the enzymatic activity of selected key enzymes involved in glucose metabolism in plaque macrophages and SMCs. Notably, two key TCA cycle dehydrogenases, SDH and IDH, exhibited minimal activity in the arterial wall and atherosclerotic plaques, whereas a heterogeneous LDH activity was observed in both the medial and intimal layers of atherosclerotic lesions. Interestingly, G6PD activity was mostly confined to the medial layer with a moderate activity found within the SMCs residing along the fibrous cap. Additionally, we observed that the uptake of [^{3}H]2-deoxyglucose had only a modest correlation with the *in situ* LDH activity, suggesting a weak association between [^{18}F]FDG uptake and the glycolytic state of atherosclerotic plaques. However, [^{3}H]2-deoxyglucose did not significantly correlate with G6PD activity.

Despite extensive investigations of PET in atherosclerosis and the growing recognition of the critical roles of immunometabolic processes in regulating various aspects of cell

biology,[1,17] most of our knowledge on the biological correlates of [^{18}F]FDG uptake in atherosclerosis has originated from *in vitro* cell culture studies[1,5,6,8,10,18] that do not accurately mimic the complex microenvironment of the vessel wall.

The microenvironment of atherosclerotic plaques is highly complex, involving multiple interconnected mechanisms that contribute to cellular metabolic heterogeneity.[1] Different cells within plaques, such as macrophages and SMCs, exhibit diverse activation states and metabolic profiles. For example, macrophages are highly plastic cells that may exist across a spectrum of activation states as exemplified by the *in vitro* concept of M1 (pro-inflammatory) and M2 (anti-inflammatory) polarization states.[1] Similarly, SMCs transition across a spectrum from a differentiated contractile phenotype in the medial layer of the arterial wall to a synthetic phenotype in the intima.[19] Local variations in oxygenation, nutrient levels, interactions with neighboring cells, and the composition of noncellular components (eg, extracellular matrix proteins, cytokines, and growth factors) as well as the mechanical forces and shear stress from blood flow create a dynamic microenvironment which influences the metabolic landscape of cells within atherosclerotic plaques.[1,20–22] Therefore, the current study attempts to address the limitation of metabolic studies performed in cultured cells in recapitulating the complexity of the plaque environment. We utilized combined *in situ* mapping of the activity of selected key enzymes involved in glucose utilization along with immunohistology to determine the activity of a few key enzymes involved in glucose utilization in SMCs and macrophages of murine and human atherosclerotic plaques. This approach enables to determine a spatial map of the metabolic heterogeneity of the cells; and therefore complements the growing strategies that delineate the cellular heterogeneity of plaques, such as single-cell RNA sequencing,[23,24] spatial transcriptomics,[25] and mass spectrometry imaging.[3] It is noteworthy that metabolism is largely regulated at posttranscriptional and posttranslational levels; hence, the assessment of enzymatic activities provides a more proximate measure of the activity of the metabolic pathways.

A major highlight of this study is the minimal activity of two key TCA cycle dehydrogenases (SDH and IDH) along with a high glycolytic activity in atherosclerotic plaques. This resembles the previously reported immunometabolic response of macrophages to lipopolysaccharide, characterized by breaks in the TCA cycle activity along with augmented glycolysis which promotes a pro-inflammatory response (eg, high interleukin-1β production) through the accumulation of succinate and stabilization of hypoxia-inducible factor-α.[26,27] Oxidative metabolism has also been linked to the inflammation-resolving state of macrophages in cell culture studies.[5,6,28] Therefore, it may be speculated that sustained glycolysis along with a low level of TCA cycle activity in plaques may promote proinflammatory activation of macrophages and/or their inefficient polarization into inflammation-resolving states; hence, contributing to the chronic nonresolving inflammation as a hallmark of atherogenesis.[29] The implications of metabolic heterogeneity of plaques for understanding the pathogenesis of atherosclerosis and the development of diagnostic/therapeutic approaches require further investigation.

Another important finding of this study was that the activity of G6PD, the rate-limiting enzyme of the oxidative PPP, was highest within the medial SMCs followed by a modest activity by fibrous cap SMCs. PPP as the main source of NADPH plays a major role in regulating the redox state of the cells by contributing to the regeneration of reduced glutathione and as a substrate for NADPH oxidases.[30] Increased G6PD activity promotes the viability of the vascular SMCs and reduces their apoptosis by improving glutathione homeostasis.[31] PPP also plays a crucial role in supporting cell proliferation by supplying ribose-5-phosphate, a key precursor for nucleotide synthesis.[32] Increased G6PD activity and glucose metabolism through PPP have been observed in proliferating vascular SMCs.[33] While it may be speculated that PPP activity may contribute to the phenotypic changes in vascular SMCs, particularly upon the activation to the synthetic phenotype, or to the integrity of the fibrous cap, the mechanistical significance of PPP in atherosclerosis and plaque vulnerability requires further investigation.

PET is a robust technique for *in vivo* imaging of vessel wall metabolism.[1] Among multiple substrates, such as ^{11}C-acetate,[7,34] (2S,4R)-4-[^{18}F]fluoroglutamine,[35] [^{18}F]fluoromethylcholine,[36] and [^{11}C]choline,[37] which have been successfully utilized for PET imaging of atherosclerosis, [^{18}F]FDG is the most extensively studied radiotracer due to its widespread availability.[1] However, the biological basis of [^{18}F]FDG PET in atherosclerosis and its clinical implications has remained incompletely understood. This reflects the limited specificity of [^{18}F]FDG as a surrogate for glucose, a ubiquitous metabolite involved in numerous metabolic pathways, as well as the scarcity of studies examining the histological correlates of [^{18}F]FDG uptake within the vessel wall. For example, while increased [^{18}F]FDG uptake has been broadly considered to be mostly driven by the increased glycolytic activity of the proinflammatory M1 polarized macrophages,[1] recent studies have shown that SMCs[4] and inflammation-resolving M2 polarized macrophages[5,6] may have a comparably high contribution to [^{18}F]FDG uptake in atherosclerotic plaques. Furthermore, the results of the current study showed only a modest association between the 2-deoxyglucose uptake and LDH activity, suggesting that the contribution of nonglycolytic utilization pathways of glucose metabolism should be considered in the interpretation of the [^{18}F]FDG PET in atherosclerosis. Notably, a comprehensive radiometabolite study has recently shown that metabolic pathways downstream of [^{18}F]FDG-6-phosphate, such as oxidative PPP, can significantly contribute to the tissue accumulation of the radioactivity reaching up to 28% at 1 h and 39% at 2 h.[38]

Metabolism has been a major focus of research over the past decade for its role in the pathogenesis of a wide range

of diseases, including cancer and cardiovascular diseases.[1,17,32,39] Beyond its significance for imaging, metabolism is increasingly being recognized as a key target for therapeutic interventions.[40] A growing body of evidence supports that several drugs currently used to reduce the risk of atherosclerosis and cardiovascular diseases, such as statins, achieve their effects by reducing inflammation through modulation of immunometabolism.[40] However, the impact of these therapeutic interventions on the heterogeneous metabolism of different cellular components of plaques has not been adequately characterized. The *in situ* assessment of cell metabolism may provide novel insights into the mechanisms by which these drugs modulate the risk of atherosclerosis and may ultimately pave the way for new therapeutic interventions that target immunometabolism.

A limitation of the current study is that *in situ* assessment of the enzymatic activities does not fully recapitulate the *in vivo* metabolism, which is regulated by various microenvironmental factors, such as the tissue oxygenation level, substrate availability, and hormonal factors. Furthermore, mapping of the activity of selected enzymes cannot provide a complete picture of the metabolic flux through a pathway. Nevertheless, *in situ* enzyme histochemistry provides a new complementary tool to the existing armamentarium to study plaque metabolism, particularly the metabolic heterogeneity of the different cellular components across different regions of the plaques. It is important to note that this study focused on delineating the metabolic heterogeneity of cells within atherosclerotic plaques, providing the biological basis for [^{18}F]FDG uptake and underscoring that [^{18}F]FDG uptake cannot simply be attributed to the pro-inflammatory activation of plaque macrophages. However, several technical limitations of PET hinder its applicability for noninvasive high-resolution mapping of plaque metabolism. First, the spatial resolution of PET is generally in the 3-5 mm range,[41] precluding cellular-level resolution. Second, high blood pool activity following [^{18}F]FDG administration impacts the accuracy of quantifying tracer uptake by the arterial wall, though advances in PET technology with the new-generation total-body scanners and dynamic imaging have improved the resolution and distinction between blood pool and vessel wall activity.[41,42] Third, arterial wall motion during the cardiac cycle deteriorates image quality and affects the accuracy of [^{18}F]FDG uptake quantification by plaques.[43] Lastly, [^{18}F]FDG uptake by myocardium is a significant challenge for detecting and quantifying its uptake by atherosclerotic plaques in the coronary arteries.[44] Consequently, extensive efforts over the past decade have focused on detecting various aspects of atherogenesis using other radiotracers. For example, fluorine-18-labeled sodium fluoride ([^{18}F]NaF) is a highly promising and readily available radiotracer for detecting calcification, a key pathogenic process in atherogenesis, in coronary arteries and other arterial beds.[45]

In summary, this study underscores the remarkably diverse metabolic activities present within atherosclerotic plaques which may not be accurately captured by *in vitro* investigation of the individual cell components. A comprehensive multidimensional approach, extending from well-regulated *in vitro* conditions (such as stable isotope metabolic tracing of cultured cells) to *in vivo* metabolic studies, is crucial to gain a deeper insight into the metabolic intricacies of various cell components within the vessel wall. Unraveling the metabolic complexities of the vessel wall may ultimately provide novel opportunities for the diagnosis and treatment of atherosclerosis.

Abbreviations

[^{18}F]FDG	2-deoxy-2-[^{18}F]fluoro-D-glucose
[^{3}H]2-deoxyglucose	2-deoxy-D-[1,2-^{3}H]glucose
α-SMA	α-smooth muscle actin
G6PD	Glucose-6-phosphate dehydrogenase
IDH	Isocitrate dehydrogenase
LDH	Lactate dehydrogenase
NAD^+	Nicotinamide adenine dinucleotide
$NADP^+$	Nicotinamide adenine dinucleotide phosphate
PET	Positron emission tomography
PPP	Pentose phosphate pathway
SDH	Succinate dehydrogenase
SMC	Smooth muscle cell
TCA	Tricarboxylic acid

Data and Materials Availability

The data needed to evaluate the conclusions of the paper are present in the paper and/or the Supplemental Materials.

Declaration of Conflicting Interests

The authors declared no potential conflicts of interest with respect to the research, authorship, and/or publication of this article.

Ethical Approval

Animal experiments were conducted in accordance with a protocol approved by the University of Pittsburgh Institutional Animal Care and Use Committee. Anonymized atherosclerotic plaques were collected from patients who underwent standard-of-care carotid endarterectomy under a "No Human Subject involvement" classification by the University of Pittsburgh Institutional Review Board. Considering the No Human Subject designation, informed consent was not required for this study.

Funding

The authors disclosed receipt of the following financial support for the research, authorship, and/or publication of this article: This study was supported by grants from the National Institute of Health (NHLBI, K08 HL144911) and Radiological Society of North America (RSD-1820) as well as a Seed Fund from University of Pittsburgh/UPMC Departments of Radiology and Medicine to S.T.

ORCID iD

Sina Tavakoli https://orcid.org/0000-0003-0574-3914

Supplemental Material

Supplemental material for this article is available online.

References

1. Mannes PZ, Tavakoli S. Imaging immunometabolism in atherosclerosis. *J Nucl Med*. 2021;62(7):896-902. doi:10.2967/jnumed.120.245407
2. Tabas I, Bornfeldt KE. Intracellular and intercellular aspects of macrophage immunometabolism in atherosclerosis. *Circ Res*. 2020;126(9):1209-1227. doi:10.1161/CIRCRESAHA.119.315939
3. Guillermier C, Doherty SP, Whitney AG, et al. Imaging mass spectrometry reveals heterogeneity of proliferation and metabolism in atherosclerosis. *JCI Insight*. 2019;4(11). doi:10.1172/jci.insight.128528
4. Al-Mashhadi RH, Tolbod LP, Bloch LO, et al. (18) Fluorodeoxyglucose accumulation in arterial tissues determined by PET signal analysis. *J Am Coll Cardiol*. 2019;74(9):1220-1232. doi:10.1016/j.jacc.2019.06.057
5. Tavakoli S, Short JD, Downs K, et al. Differential regulation of macrophage glucose metabolism by macrophage colony-stimulating factor and granulocyte-macrophage colony-stimulating factor: implications for (18)F FDG PET imaging of vessel wall inflammation. *Radiology*. 2017;283(1):87-97. doi:10.1148/radiol.2016160839
6. Tavakoli S, Zamora D, Ullevig S, et al. Bioenergetic profiles diverge during macrophage polarization: implications for the interpretation of 18F-FDG PET imaging of atherosclerosis. *J Nucl Med*. 2013;54(9):1661-1667. doi:10.2967/jnumed.112.119099
7. Demirdelen S, Mannes PZ, Aral AM, et al. Divergence of acetate uptake in proinflammatory and inflammation-resolving macrophages: implications for imaging atherosclerosis. *J Nucl Cardiol*. 2022;29(3):1266-1276. doi:10.1007/s12350-020-02479-5
8. Tavakoli S, Downs K, Short JD, et al. Characterization of macrophage polarization states using combined measurement of 2-deoxyglucose and glutamine accumulation: implications for imaging of atherosclerosis. *Arterioscler Thromb Vasc Biol*. 2017;37(10):1840-1848. doi:10.1161/ATVBAHA.117.308848
9. Folco EJ, Sheikine Y, Rocha VZ, et al. Hypoxia but not inflammation augments glucose uptake in human macrophages: implications for imaging atherosclerosis with 18fluorine-labeled 2-deoxy-D-glucose positron emission tomography. *J Am Coll Cardiol*. 2011;58(6):603-614. doi:10.1016/j.jacc.2011.03.044
10. Lee SJ, Thien Quach CH, Jung KH, et al. Oxidized low-density lipoprotein stimulates macrophage 18F-FDG uptake via hypoxia-inducible factor-1alpha activation through Nox2-dependent reactive oxygen species generation. *J Nucl Med*. 2014;55(10):1699-1705. doi:10.2967/jnumed.114.139428
11. Miller A, Nagy C, Knapp B, et al. Exploring metabolic configurations of single cells within complex tissue microenvironments. *Cell Metab*. 2017;26(5):788-800.e6. doi:10.1016/j.cmet.2017.08.014
12. Molenaar RJ, Khurshed M, Hira VVV, Van Noorden CJF. Metabolic mapping: quantitative enzyme cytochemistry and histochemistry to determine the activity of dehydrogenases in cells and tissues. *J Vis Exp*. 2018;135. doi:10.3791/56843
13. Talaiezadeh A, Shahriari A, Tabandeh MR, Fathizadeh P, Mansouri S. Kinetic characterization of lactate dehydrogenase in normal and malignant human breast tissues. *Cancer Cell Int*. 2015;15(1):19. doi:10.1186/s12935-015-0171-7
14. Tiwari M. Glucose 6 phosphatase dehydrogenase (G6PD) and neurodegenerative disorders: mapping diagnostic and therapeutic opportunities. *Genes Dis*. 2017;4(4):196-203. doi:10.1016/j.gendis.2017.09.001
15. Yellen G. Fueling thought: management of glycolysis and oxidative phosphorylation in neuronal metabolism. *J Cell Biol*. 2018;217(7):2235-2246. doi:10.1083/jcb.201803152
16. Parra-Bonilla G, Alvarez DF, Al-Mehdi AB, Alexeyev M, Stevens T. Critical role for lactate dehydrogenase A in aerobic glycolysis that sustains pulmonary microvascular endothelial cell proliferation. *Am J Physiol Lung Cell Mol Physiol*. 2010;299(4):L513-L522. doi:10.1152/ajplung.00274.2009
17. van Tuijl J, Joosten LAB, Netea MG, Bekkering S, Riksen NP. Immunometabolism orchestrates training of innate immunity in atherosclerosis. *Cardiovasc Res*. 2019;115(9):1416-1424. doi:10.1093/cvr/cvz107
18. Singh P, Gonzalez-Ramos S, Mojena M, et al. GM-CSF enhances macrophage glycolytic activity in vitro and improves detection of inflammation in vivo. *J Nucl Med*. 2016;57(9):1428-1435. doi:10.2967/jnumed.115.167387
19. Allahverdian S, Chaabane C, Boukais K, Francis GA, Bochaton-Piallat M-L. Smooth muscle cell fate and plasticity in atherosclerosis. *Cardiovasc Res*. 2018;114(4):540-550. doi:10.1093/cvr/cvy022
20. Stroope C, Nettersheim FS, Coon B, et al. Dysregulated cellular metabolism in atherosclerosis: mediators and therapeutic opportunities. *Nat Metab*. 2024;6(4):617-638. doi:10.1038/s42255-024-01015-w
21. Hou P, Fang J, Liu Z, et al. Macrophage polarization and metabolism in atherosclerosis. *Cell Death Dis*. 2023;14(10):691. doi:10.1038/s41419-023-06206-z
22. Jiang M, Ding H, Huang Y, Wang L. Shear stress and metabolic disorders-two sides of the same plaque. *Antioxid Redox Signal*. 2022;37(10-12):820-841. doi:10.1089/ars.2021.0126
23. Alsaigh T, Evans D, Frankel D, Torkamani A. Decoding the transcriptome of calcified atherosclerotic plaque at single-cell resolution. *Commun Biol*. 2022;5(1):1084. doi:10.1038/s42003-022-04056-7
24. Vallejo J, Cochain C, Zernecke A, Ley K. Heterogeneity of immune cells in human atherosclerosis revealed by scRNA-Seq. *Cardiovasc Res*. 2021;117:2537-2543. doi:10.1093/cvr/cvab260
25. Sun J, Singh P, Shami A, et al. Spatial transcriptional mapping reveals site-specific pathways underlying human atherosclerotic plaque rupture. *J Am Coll Cardiol*. 2023;81(23):2213-2227. doi:10.1016/j.jacc.2023.04.008
26. Jha AK, Huang SC, Sergushichev A, et al. Network integration of parallel metabolic and transcriptional data reveals metabolic modules that regulate macrophage polarization. *Immunity*. 2015;42(3):419-430. doi:10.1016/j.immuni.2015.02.005
27. Tannahill GM, Curtis AM, Adamik J, et al. Succinate is an inflammatory signal that induces IL-1beta through HIF-1alpha. *Nature*. 2013;496(7444):238-242. doi:10.1038/nature11986
28. Wculek SK, Dunphy G, Heras-Murillo I, Mastrangelo A, Sancho D. Metabolism of tissue macrophages in homeostasis and pathology. *Cell Mol Immunol*. 2022;19(3):384-408. doi:10.1038/s41423-021-00791-9
29. Fredman G, MacNamara KC. Atherosclerosis is a major human killer and non-resolving inflammation is a prime suspect. *Cardiovasc Res*. 2021;117:2563-2574. doi:10.1093/cvr/cvab309
30. Shi J, Yang Y, Cheng A, Xu G, He F. Metabolism of vascular smooth muscle cells in vascular diseases. *Am J Physiol Heart*

Circ Physiol. 2020;319(3):H613-H631. doi:10.1152/ajpheart.00220.2020
31. Dong LH, Li L, Song Y, et al. TRAF6-mediated SM22alpha K21 ubiquitination promotes G6PD activation and NADPH production, contributing to GSH homeostasis and VSMC survival in vitro and in vivo. *Circ Res*. 2015;117(8):684-694. doi:10.1161/CIRCRESAHA.115.306233
32. Jiang P, Du W, Wu M. Regulation of the pentose phosphate pathway in cancer. *Protein Cell*. 2014;5(8):592-602. doi:10.1007/s13238-014-0082-8
33. Dhagia V, Kitagawa A, Jacob C, et al. G6PD activity contributes to the regulation of histone acetylation and gene expression in smooth muscle cells and to the pathogenesis of vascular diseases. *Am J Physiol Heart Circ Physiol*. 2021;320(3):H999-H1016. doi:10.1152/ajpheart.00488.2020
34. Derlin T, Habermann CR, Lengyel Z, et al. Feasibility of 11C-acetate PET/CT for imaging of fatty acid synthesis in the atherosclerotic vessel wall. *J Nucl Med*. 2011;52(12):1848-1854. doi:10.2967/jnumed.111.095869
35. Palani S, Miner MWG, Virta J, et al. Exploiting glutamine consumption in atherosclerotic lesions by positron emission tomography tracer (2S,4R)-4-(18)F-fluoroglutamine. *Front Immunol*. 2022;13:821423. doi:10.3389/fimmu.2022.821423
36. Bucerius J, Schmaljohann J, Bohm I, et al. Feasibility of 18F-fluoromethylcholine PET/CT for imaging of vessel wall alterations in humans–first results. *Eur J Nucl Med Mol Imaging*. 2008;35(4):815-820. doi:10.1007/s00259-007-0685-x
37. Kato K, Schober O, Ikeda M, et al. Evaluation and comparison of 11C-choline uptake and calcification in aortic and common carotid arterial walls with combined PET/CT. *Eur J Nucl Med Mol Imaging*. 2009;36(10):1622-1628. doi:10.1007/s00259-009-1152-7
38. Patronas EM, Balber T, Miller A, et al. A fingerprint of 2-[(18)F]FDG radiometabolites - how tissue-specific metabolism beyond 2-[(18)F]FDG-6-P could affect tracer accumulation. *iScience*. 2023;26(11):108137. doi:10.1016/j.isci.2023.108137
39. Geeraerts X, Fernandez-Garcia J, Hartmann FJ, et al. Macrophages are metabolically heterogeneous within the tumor microenvironment. *Cell Rep*. 2021;37(13):110171. doi:10.1016/j.celrep.2021.110171
40. Ketelhuth DFJ, Lutgens E, Back M, et al. Immunometabolism and atherosclerosis: Perspectives and clinical significance: A position paper from the Working Group on Atherosclerosis and Vascular Biology of the European Society of Cardiology. *Cardiovasc Res*. 2019;115(9):1385-1392. doi:10.1093/cvr/cvz166
41. Derlin T, Spencer BA, Mamach M, et al. Exploring vessel wall biology in vivo by ultrasensitive total-body PET. *J Nucl Med*. 2023;64(3):416-422. doi:10.2967/jnumed.122.264550
42. Derlin T, Werner RA, Weiberg D, Bengel FM. Parametric imaging of biologic activity of atherosclerosis using dynamic whole-body positron emission tomography. *JACC Cardiovasc Imaging*. 2022;15(12):2098-2108. doi:10.1016/j.jcmg.2022.05.008
43. Tavakoli S. Technical considerations for quantification of (18)F-FDG uptake in carotid atherosclerosis. *J Nucl Cardiol*. 2019;26(3):894-898. doi:10.1007/s12350-017-1060-3
44. Tavakoli S, Vashist A, Sadeghi MM. Molecular imaging of plaque vulnerability. *J Nucl Cardiol*. 2014;21(6):1112-1128; quiz 1129. doi:10.1007/s12350-014-9959-4
45. Ng SJ, Lau HC, Naseer R, et al. Atherosclerosis imaging: positron emission tomography. *PET Clin*. 2023;18(1):71-80. doi:10.1016/j.cpet.2022.09.004